as the cell voltage decreases during discharge. The discharge behavior is governed here by the long time constant of the electrometer, but with slower redox couples it would also be governed by the heterogeneous electron-transfer kinetics. For example, at an electrode of radius a (nanometers) in a solution containing C^b (micromolar concentrations) redox couple with a heterogeneous electron-transfer rate constant k_s (centimeters per second), the number of net oxidative charge-transfer events, N_{CTE} (hertz), at low overpotential η, assuming the transfer coefficient $\alpha = 0.5$, is given by

$$N_{CTE} = 7.36 \times 10^2 a^2 k_s C^b \eta \qquad (6)$$

Thus for a 1 μM redox couple having slow charge-transfer kinetics, for example, k_s = 0.001 cm/s, it takes an average of ~25 s for a single electron-transfer event to occur at η = 9 mV at an electrode of radius 2.5 nm.

These coulomb staircase measurements show that nanometer-size structures can be produced without high-resolution lithographic processing or precise positioning of electrode tips. As with other single molecule processes, they may find use in the study of environmental effects on electron transfers and in determination of the heterogeneous kinetics of rapid electron-transfer reactions.

REFERENCES AND NOTES

1. F.-R. F. Fan and A. J. Bard, *Science* **267**, 871 (1995); F.-R. F. Fan, J. Kwak, A. J. Bard, *J. Am. Chem. Soc.* **118**, 9669 (1996).
2. M. M. Collison and R. M. Wightman, *Science* **268**, 1883 (1995).
3. F.-R. F. Fan and A. J. Bard, *Acc. Chem. Res.* **29**, 572 (1996).
4. Reviewed by H. Grabert and M. H. Devoret, Eds., *Single Charge Tunneling* (Plenum, New York, 1992); M. A. Kastner, *Phys. Today* **46**, 24 (January 1993).
5. I. O. Kulik and R. I. Shekhter, *Sov. Phys. JETP* **41**, 308 (1975).
6. M. Amman, R. Wilkins, E. Ben-Jacob, P. D. Maker, R. C. Jaklevic, *Phys. Rev. B* **43**, 1146 (1991).
7. A. E. Hanna and M. Tinkham, *ibid.* **44**, 5919 (1991).
8. M. Bockrath *et al.*, *Science* **275,** 1922 (1997).
9. R. P. Andres *et al.*, *ibid.* **272**, 1323 (1996).
10. L. Guo, E. Leobandung, S. Y. Chou, *ibid.* **275**, 649 (1997).
11. All current or voltage measurements were carried out at room temperature (25.0° ± 0.5°C) with a deaerated solution with a Keithley Model 617 electrometer. Current was found from the potential drop across the nominally 200-Tohm internal resistance at the most sensitive voltage setting. The leads were connected in the guard mode with the inner shield connected to the ungrounded electrode lead. The cell was placed inside a grounded Faraday cage.
12. L. A. Nagahara, T. Thundat, S. M. Lindsey, *Rev. Sci. Instrum.* **60**, 3128 (1989); M. V. Mirkin, F.-R. F. Fan, A. J. Bard, *J. Electroanal. Chem.* **328**, 47 (1992). Insulation of the tip was done with low–melting point polyethylene or Apiezon wax. The insulated tip was then mounted on a scanning electrochemical microscope (SECM) in a cell containing 1 mM Cp_2FeTMA^+ and 1 M $NaNO_3$. The very end of the tip was then exposed by applying 0.60 V versus saturated calomel electrode on the tip and −0.20 V on a conductive substrate (such as indium tin oxide, ITO) with the SECM operated in the constant current mode (with a reference current of 10 pA). As the well-insulated tip approached the surface of the substrate, the onset of an enhanced current flow caused the z-piezo to retract the tip. This process produced a hole in the tip insulation at the point of closest approach of tip to substrate while leaving most of the tip still insulated.
13. Y. Saito, *Rev. Polarogr.* **15**, 177 (1969).
14. A. J. Bard and L. R. Faulkner, *Electrochemical Methods* (Wiley, New York, 1980), p. 322.
15. Here we treat the electrochemical system (having a voltage V_{corr}) and the input shunt capacitor (having a voltage V_m) of the electrometer as two voltage sources coupled in parallel. Thus, the combined voltage (that is, the observed voltage V_u) is given by $(V_{corr} + V_m)/2$ or $V_{corr} = 2V_u - V_m$.

16. Supported by the Robert A. Welch Foundation and the National Science Foundation.

9 May 1997; accepted 22 July 1997

Solvophobically Driven Folding of Nonbiological Oligomers

James C. Nelson,* Jeffery G. Saven,† Jeffrey S. Moore, Peter G. Wolynes

In solution, biopolymers commonly fold into well-defined three-dimensional structures, but only recently has analogous behavior been explored in synthetic chain molecules. An aromatic hydrocarbon backbone is described that spontaneously acquires a stable helical conformation having a large cavity. The chain does not form intramolecular hydrogen bonds, and solvophobic interactions drive the folding transition, which is sensitive to chain length, solvent quality, and temperature.

Proteins and polynucleotides epitomize intramolecular self-organization in solution, as is evidenced by their spontaneous and reversible folding into well-defined conformations (*1*). A flexible biopolymer may assume many conformations, and entropic effects favor the absence of internal order. The folded state, however, is stabilized by a variety of noncovalent cohesive forces, including hydrogen (H) bonds, electrostatic forces, steric packing, and hydrophobic effects (*2*). Given the complexity of biopolymers, unraveling the respective roles of the entropic and energetic interactions remains a challenging area of theoretical (*3*) and experimental (*4*) research. Nonbiological macromolecules, however, may provide simpler systems for investigating self-organization and allow researchers to isolate particular interactions. In addition, the folding of linear polymers may provide synthetically simple means of generating architectures that could potentially rival the biopolymers in their complexity and functionality. One of the best studied folding motifs is the single-stranded helix, which can also serve as the basis for more complicated structures, as it does in proteins. In this report, we theoretically and experimentally characterize a nonbiological, supramolecular helix-forming oligomer.

Much emphasis has been placed on the role of H bonds in stabilizing secondary structures, ever since these structures were predicted in proteins on that basis (*5*). Many have argued that the primary reason that proteins fold is due to intramolecular H bonding of the backbone (*6*). Similarly, most attempts to create synthetic polymers with secondary structure have involved the engineering of H bonds, where the backbones used have been closely related to peptides (*7, 8*). However, H-bonded structures that are stable in nonpolar solvents often disintegrate in aqueous solution because of solvent competition (*7*). In proteins, hydrophobic interactions and compaction due to hydrophobic collapse undoubtedly also play a role in guiding helix formation (*9, 10*). Unlike H bonds, hydrophobic and van der Waals interactions are less selective and directionally specific, which discourages their use to confer conformational uniqueness. Given the substantial experimental focus on understanding H bonds in proteins and engineering them in synthetic polymers, we have chosen to investigate the extent to which nonspecific forces alone can guide intramolecular self-organization.

Although soluble ordered structures that are not largely H bonded have been obtained (*11*), here we report the folding of a phenylacetylene oligomer (Fig. 1A) whose cooperative transition can be driven, just as for proteins, by both solvent and temperature changes. The oligomer is guided to a folded, helical conformation by nondirectional interactions and local constraints caused by the covalent structure of the

J. C. Nelson and J. S. Moore, Departments of Chemistry and Materials Science and Engineering and the Beckman Institute for Advanced Science and Technology, University of Illinois, Urbana, IL 61801, USA.
J. G. Saven and P. G. Wolynes, School of Chemical Sciences, University of Illinois, Urbana, IL 61801, USA.

*Present address: Glaxo Wellcome, Five Moore Drive, Post Office Box 13398, Research Triangle Park, NC 27709, USA.
†Present address: Department of Chemistry, University of Pennsylvania, Philadelphia, PA 19104, USA.

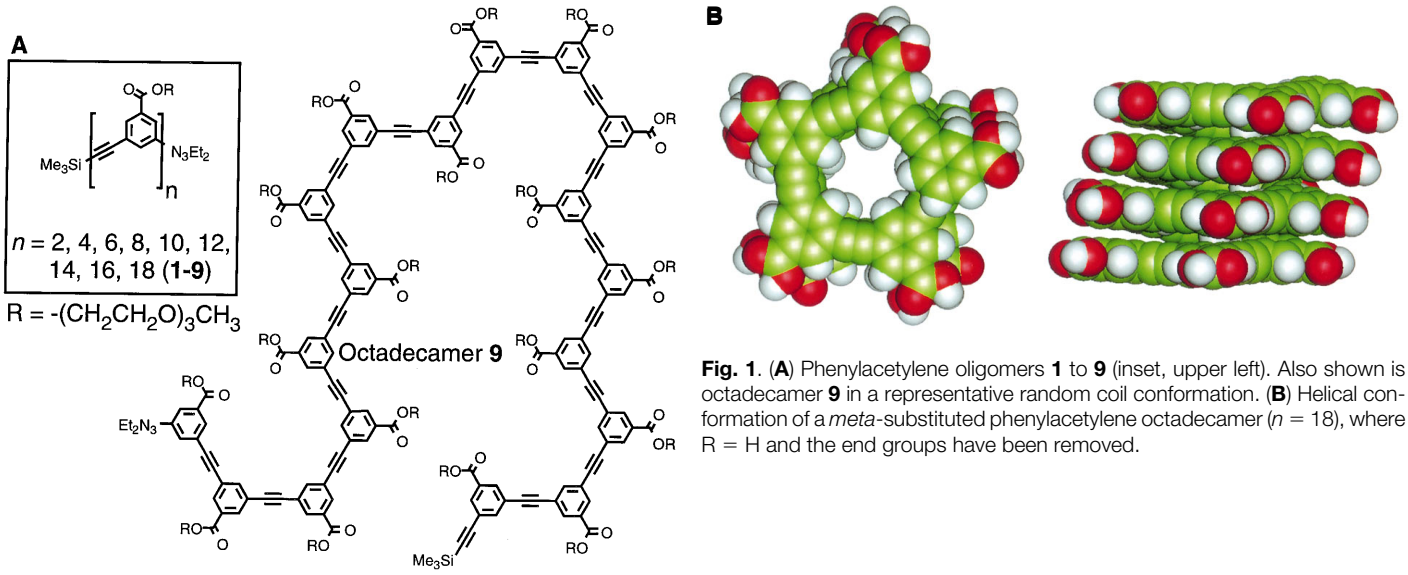

Fig. 1. (**A**) Phenylacetylene oligomers **1** to **9** (inset, upper left). Also shown is octadecamer **9** in a representative random coil conformation. (**B**) Helical conformation of a *meta*-substituted phenylacetylene octadecamer (n = 18), where R = H and the end groups have been removed.

backbone. A substantial number of open chain conformations are available to an all-*meta* phenylacetylene oligomer, whereas the compact helical conformation has a well-defined tubular cavity that is potentially useful for binding (Fig. 1B).

Computational studies suggest the possibility of self-organization. Chain lengths at which the fully helical conformation becomes stable were estimated with molecular mechanics and the microscopic theory of the helix-coil transition (*12*, *13*). We calculated the difference in free energy (ΔG) between the helically ordered state and the ensemble of unfolded conformations. To simplify these calculations, we considered chains having benzoate end groups and rudimentary side chains (see Fig. 1B). The length of an oligomer refers to n, the number of benzene rings per molecule. The onset of helical stability ($\Delta G < 0$) is predicted to occur at similar chain lengths (n) of 7 and 8 for two different side chains in two very different solvents: carboxylic acid oligomers (R = H) in water and methyl benzoate oligomers (R = CH_3) in chloroform (Fig. 2).

We synthesized soluble oligomers (dimer **1** through octadecamer **9**) (*14*) whose chain lengths span this onset of helical stability (Fig. 1A). Oligomers bearing the triglyme mono methyl ether group [R = $(CH_2CH_2O)_3CH_3$] are soluble in a number of different solvents, including chloroform, acetonitrile, and acetonitrile-water mixtures.

The hypochromic effect is a powerful indicator of the oriented chromophores commonly seen in DNA, RNA, and other polymers (*15*, *16*), where the effect is observed as the reduction in optical ab-

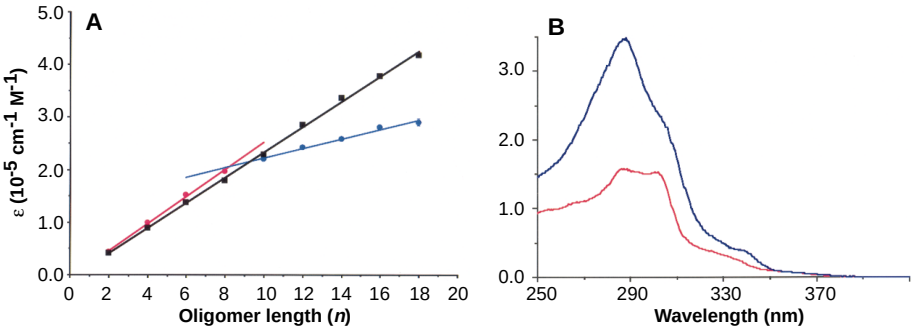

Fig. 3. (A) The molar extinction coefficient ε (303 nm) versus oligomer length n for oligomers **1** to **9** in chloroform (black) and acetonitrile (red and blue). The lines are linear fits to the data; for acetonitrile, the fits are for n = 2 to 8 (red) and n = 10 to 18 (blue). (**B**) Representative UV spectra in acetonitrile: hexamer **3** (red) and dodecamer **6** (blue).

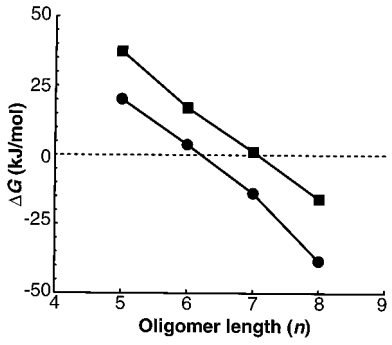

Fig. 2. Estimated free energy of helix formation Δ*G* versus chain length for *meta*-substituted oligomers at 27°C. Squares, methyl benzoate–substituted oligomers (R = CH_3) in chloroform; circles, carboxylic acid–substituted oligomers (R = H) in water.

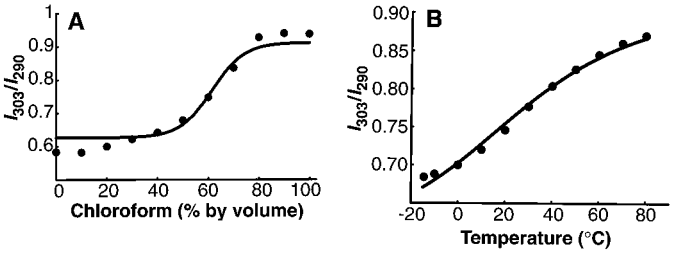

Fig. 4. (**A**) The ratio of the intensities of the UV absorption maxima at 290 and 303 nm (I_{303}/I_{290}) versus percent of chloroform in acetonitrile (by volume) at 25°C for octadecamer **9**. (**B**) I_{303}/I_{290} versus temperature (T) for octadecamer **9** in 60% chloroform. The curves in (A) and (B) are fits to a simple all-or-none two-state model of the helix-coil equilibria (*12*), where the equilibrium constant is $K_{eq} = \sigma s^{n-5}$, σ and s are the helix nucleation and growth parameters, and ln(s) is linearly dependent on the percent of chloroform (A) or $1/T$ (B). For example, $\sigma = 10^{-3}$ and $s = 3$ in acetonitrile at 25°C. The spectra were measured at micromolar concentrations.

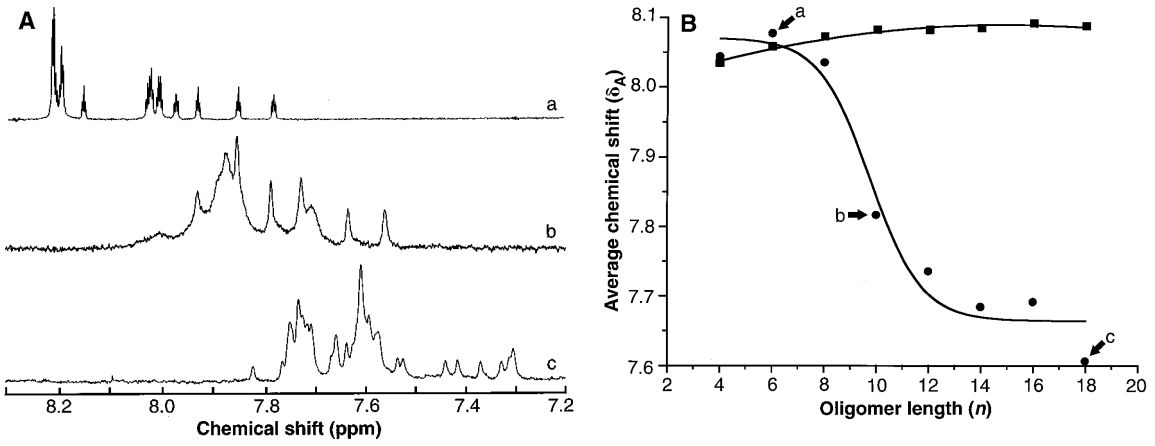

Fig. 5. (**A**) The ^{1}H NMR (750 MHz) spectra in acetonitrile for hexamer **3** (a), decamer **5** (b), and octadecamer **9** (c) at 25°C. (**B**) The average chemical shift δ_A versus chain length *n* for oligomers **1** to **9** in chloroform ($CDCl_3$) (squares) and acetonitrile (CD_3CN) (circles) (*21*). The curves are drawn only as guides to the eye. All the spectra in chloroform and those of **1** to **4** in acetonitrile did not change upon dilution; the spectra of **5** to **9** in acetonitrile were measured at ~10 μM (*22*).

sorption intensity. Hypochromic effects are sensitive to the distance *r* between chromophores (varying as r^{-3}) and their relative orientations (*15*). In the absence of any helical ordering, the molar extinction coefficient ε (303 nm) should be linearly dependent on oligomer length, because the effective concentration of chromophores increases linearly with chain size. If we assume that effects due to the acetylenic backbone and the side chains are negligible, monomer chromophores in the helix will be aligned in a fashion that diminishes the overall absorption, and ε will fall below the linear extrapolation based on shorter chains that are incapable of forming helices. For oligomers **1** to **9** in chloroform, ε is linearly dependent on *n* over the entire range of oligomer lengths (Fig. 3A). However, in acetonitrile ε changes abruptly in its chain length dependence near $n = 8$. For $n > 8$, ε is also linearly dependent on *n*, but the slope is 35% that seen for the shorter oligomers (Fig. 3A). To rule out intermolecular association, ε for each oligomer was determined by using a range of concentrations. For each compound, Beer's law behavior was observed. Thus the hypochromic shifts arise from purely intramolecular interactions. These results indicate that the oligomers with $n > 8$ in acetonitrile are in an ordered conformation consistent with helix formation.

The shapes of the ultraviolet (UV) spectra of the oligomers are sensitive to chain length, solvent, and temperature (Fig. 3B). For all of the oligomers in chloroform and the shorter oligomers in acetonitrile, two peaks of nearly equal intensity appear at 290 and 303 nm, but for $n > 10$ in acetonitrile, the intensity of the 303-nm band (I_{303}) is ~60% that of the 290-nm band (I_{290}) (*17*). In mixtures of the two solvents, the ratio of the intensities I_{303}/I_{290} for octadecamer **9** increases nonlinearly with increasing chloroform content (Fig. 4A). I_{303}/I_{290} exhibits a sharp increase centered at 60% chloroform, behavior that suggests a cooperative transition consistent with helix formation. I_{303}/I_{290} also increases with increasing temperature (Fig. 4B). To the extent that I_{303}/I_{290} quantifies the population of the fully helical state, this behavior mimics the thermal stability observed in helical peptides (*18*). The data can be fitted with a simple two-state model of the helix-coil equilibria that considers only the random coil and fully helical configurations (Fig. 4, A and B). Thus, chloroform acts as a "denaturant" (in contrast to the modeling results), and in mixed solvents the ordered oligomer can be thermally unstable.

The chemical shifts δ of the aromatic ^{1}H nuclear magnetic resonance (NMR) provide additional evidence for conformational ordering. The chemical shifts of protons within 7 Å of an aromatic ring experience an upfield shift to smaller δ when located above the ring (*19*). Thus upfield shifts in the aromatic proton resonances are consistent with parallel stacking of aromatic subunits (*20*). Provided the concentration is below the onset of intermolecular association, we can use ^{1}H NMR spectra to probe intramolecular aromatic stacking in the open chain oligomers (Fig. 5A). For dimer **1** through octadecamer **9** in chloroform at 25°C, the average chemical shift δ_A of the aromatic region of the ^{1}H NMR [7.2 to 8.3 parts per million (ppm)] exhibits only a slight downfield shift with increasing chain length (*21*) (Fig. 5B). This slight shift is due to the diminishing contribution of the end groups (trimethylsilyl and diethyl triazene) to δ_A with increasing chain size. In acetonitrile (Fig. 5B), however, δ_A shifts abruptly upfield by about 0.4 ppm as the chain length increases from 8 to 14. For chain lengths $n > 12$, δ_A is approximately constant. From independent measurements, we know that the chemical shifts observed in acetonitrile for $n > 10$ are an intramolecular effect (*22*).

We have presented the design and characterization of helix-forming oligomers whose ordered conformations are stabilized by "nonspecific" forces. The UV absorption and ^{1}H NMR spectra provide strong evidence of helix formation for $n > 8$ in acetonitrile. Intramolecular aromatic stacking maximizes solvent interactions with the polar side chains, maximizes aromatic-aromatic contacts, and minimizes interactions of the hydrocarbon backbone with solvent. In agreement with the calculations, which suggest that longer oligomers form conformationally well-defined helices, octadecamer **9** has the largest shift in δ_A and the best-resolved ^{1}H NMR spectra for $n > 12$ in acetonitrile (Fig. 5A). Not included in the calculations, however, was an entropy cost upon folding due to the loss of side chain degrees of freedom, and this must partially explain the discrepancy between the modeling and experimental results in chloroform.

When solvophobic interactions are the dominant contribution to stability, the structures of folded polymers should tolerate many modifications of the backbone and monomer types. By synthesizing these oligomers on a solid support (*23*), combinatorial experiments could probe a broad range of monomer modifications. Eventually, phenylacetylene helices could be catenated to form sophisticated architectures, which may self-organize in aqueous and nonaqueous environments. Such design schemes are likely to produce binding surfaces with the high information content necessary for molecular recognition. Lastly, these helical structures possess an ordered modifiable cavity that may be used to bind a variety of metals, small molecules, and reactive species.

REFERENCES AND NOTES

1. C. B. Anfinsen, *Science* **181**, 223 (1973).
2. P. L. Privalov, in *Protein Folding* (Freeman, New York, 1992), pp. 83–126; T. E. Creighton, *Proteins*

(Freeman, New York, 1993).
3. J. D. Bryngelson, J. N. Onuchic, N. D. Socci, P. G. Wolynes, *Proteins* **21**, 167 (1995); K. A. Dill *et al.*, *Protein Sci.* **4**, 561 (1995); L. A. Mirny, V. Abkevich, E. I. Shakhnovich, *Folding Design* **1**, 221 (1996).
4. J. W. Bryson *et al.*, *Science* **270**, 935 (1995); D. A. Dolgikh, M. P. Kirpichnikov, O. B. Ptitsyn, V. V. Chemeris, *Mol. Biol.* **30**, 149 (1996).
5. L. Pauling, R. B. Corey, H. R. Branson, *Proc. Natl. Acad. Sci. U.S.A.* **37**, 205 (1951).
6. C. M. Venkatchalam and G. N. Ramachandran, *Annu. Rev. Biochem.* **38**, 45 (1969); B. Honig and F. E. Cohen, *Folding Design* **1**, R17 (1996).
7. J.-M. Lehn, *Angew. Chem. Int. Ed. Engl.* **29**, 1304 (1990); G. M. Whitesides, J. P. Mathias, C. T. Seto, *Science* **254**, 1312 (1991); D. S. Lawrence, T. Jiang, M. Levett, *Chem. Rev.* **95**, 2229 (1995).
8. M. Hagihara, N. J. Anthony, T. J. Stout, J. Clardy, S. L. Schreiber, *J. Am. Chem. Soc.* **114**, 6568 (1992); G. P. Dado and S. H. Gellman, *ibid.* **116**, 1054 (1994); A. B. Smith *et al.*, *ibid.*, p. 9947; Y. Hamuro, S. J. Geib, A. D. Hamilton, *ibid.* **118**, 7529 (1996); D. H. Appella, L. A. Christianson, I. L. Karle, D. R. Powell, S. H. Gellman, *ibid.*, p. 13071; D. Seebach *et al.*, *Helv. Chim. Acta* **79**, 2043 (1996).
9. W. Kauzmann, *Adv. Prot. Chem.* **14**, 1 (1959); M. Bixon, H. A. Scheraga, S. Lifson, *Biopolymers* **1**, 419 (1963); S. Padmanabhan and R. L. Baldwin, *J. Mol. Biol.* **241**, 706 (1994); Z. Luthey-Schulten, B. E. Ramirez, P. G. Wolynes, *J. Phys. Chem.* **99**, 2177 (1995); J. G. Saven and P. G. Wolynes, *J. Mol. Biol.* **257**, 199 (1996).
10. A.-S. Yang and B. Honig, *J. Mol. Biol.* **252**, 351 (1995).
11. R. S. Lokey and B. L. Iverson, *Nature* **375**, 303 (1995).
12. D. Poland and H. A. Scheraga, *Theory of Helix-Coil Transitions in Biopolymers* (Academic Press, New York, 1970).
13. A modified version of the force field of Jorgensen and Tirado-Rives (*24*) was used, which included a 0.6 kcal/mol barrier to torsional rotation about the triple bond as inferred from gas-phase spectroscopy (*25*). The helix-coil free energy difference $\Delta G = G_{helix} - G_{coil}$ was estimated using Eqs. 1 and 2,

$$G_{helix} = G_{solvation} - RT \ln z_{vib} \quad (1)$$

$$G_{coil} = G_{solvation} - RT \ln z_{vib} - RT \ln \alpha_{torsion} \quad (2)$$

where G_{helix} and G_{coil} are the free energies of the helical and random coil parts of conformation space (*10, 26*). In each case, the solvent-accessible surface area of an energy-minimized helical or extended conformation was determined, and semi-empirical relations were used to map this area to a free energy of solvation, $G_{solvation}$ (*27*). For both G_{helix} and G_{coil}, the vibrational partition function z_{vib} was calculated with a normal mode analysis about the local minimum. In G_{coil}, $\alpha_{torsion}$ corrects z_{vib} to include full rotational torsion about the acetylene bridges, and these torsion angles were taken to be independent of one another. Both z_{vib} and $G_{solvation}$ were essentially identical for any of the extended, planar local minima chosen to represent the nonhelical ensemble.
14. J. Zhang, D. J. Pesak, J. L. Ludwick, J. S. Moore, *J. Am. Chem. Soc.* **116**, 4227 (1994).
15. V. A. Bloomfield, D. M. Crothers, I. Tinoco, *Physical Chemistry of Nucleic Acids* (Harper & Row, New York, 1974).
16. C. R. Cantor and P. R. Schimmel, *Biophysical Chemistry* (Freeman, New York, 1980).
17. I_{303}/I_{290} of the octadecamer **9** sample did not change upon dilution by a factor of 50. For **9** in acetonitrile, ε (290 nm) was only 12% less than the extrapolated value based on short chain lengths, which makes I_{290} a useful internal reference.
18. J. M. Scholtz, H. Aian, E. J. York, J. M. Sterward, R. L. Baldwin, *Biopolymers* **31**, 1463 (1991).
19. S. J. Perkins, *Biol. Magn. Reson.* **4**, 193 (1982).
20. A. S. Shetty, J. Zhang, J. S. Moore, *J. Am. Chem. Soc.* **118**, 1019 (1996).
21. $\delta_A = [\Sigma\, \delta\, I(\delta)]/\Sigma\, I(\delta)$, where δ is the chemical shift, $I(\delta)$ is the spectral intensity, and each sum extends only over the aromatic region of the spectrum, typically δ = 7.2 to 8.3.
22. With the use of vapor pressure osmometry, the intermolecular association constants K_a of **1** to **6** could be reliably measured in acetonitrile at 37°C. K_a increases with n: For example, K_a(**2**) = 8 ± 3 M^{-1}, K_a(**4**) = 49 ± 14 M^{-1}, and K_a(**6**) = 1186 ± 143 M^{-1}. If variation in K_a(**6**) over small changes in temperature is neglected, only ~3% of **6** is expected to be involved in bimolecular aggregates at 10 μM and 25°C. In each case, K_a was determined with a model that assumes K_a is the same for the dimer and all higher-order aggregates.
23. J. C. Nelson, J. K. Young, J. S. Moore, *J. Org. Chem.* **61**, 8160 (1996).
24. W. L. Jorgensen and J. Tirado-Rives, *J. Am. Chem. Soc.* **110**, 1657 (1988).
25. K. Okuyama, T. Hasegawa, M. Ito, N. Mikami, *J. Phys. Chem.* **88**, 1711 (1984).
26. N. Go, M. Go, H. A. Scheraga, *Proc. Nat. Acad. Sci. U.S.A.* **59**, 1030 (1968).
27. W. C. Still, A. Tempczyk, R. C. Hawley, T. Hendrickson, *J. Am. Chem. Soc.* **112**, 6127 (1990); MacroModel, v5.0 (1996) [F. Mohamadi *et al.*, *J. Comput. Chem.* **11**, 440 (1990)].
28. The authors acknowledge support from the Critical Research Initiatives Program of the University of Illinois, NSF grant CHE 94-96105 (to J.S.M.), and NSF grant CHE-93-01474 (to J.G.S.). This work was completed while P.G.W. was a Scholar-in-Residence at the Fogarty International Center at NIH. The NMR studies were funded in part from the W. M. Keck Foundation, NIH (grant PHS 1 S10 RR10444-01), and NSF (grant CHE 96-10502).

8 May 1997; accepted 24 July 1997

A Mound Complex in Louisiana at 5400–5000 Years Before the Present

Joe W. Saunders,* Rolfe D. Mandel, Roger T. Saucier, E. Thurman Allen, C. T. Hallmark, Jay K. Johnson, Edwin H. Jackson, Charles M. Allen, Gary L. Stringer, Douglas S. Frink, James K. Feathers, Stephen Williams, Kristen J. Gremillion, Malcolm F. Vidrine, Reca Jones

An 11-mound site in Louisiana predates other known mound complexes with earthen enclosures in North America by 1900 years. Radiometric, luminescence, artifactual, geomorphic, and pedogenic data date the site to over 5000 calendar years before present. Evidence suggests that the site was occupied by hunter-gatherers who seasonally exploited aquatic resources and collected plant species that later became the first domesticates in eastern North America.

Native American mounds have been recognized and studied in the eastern United States for more than a century. They represent early evidence for organized society in North America. Most of the earthen mounds and enclosures in the east date to <2500 calendar years before present (B.P.) (*1*). In the 1950s, the recognition of preceramic mounds and earthen enclosures from earlier times came first at the Poverty Point site in Louisiana, dating to 3500 calendar years B.P. (*2, 3*). By the 1970s, four mound sites in Louisiana and one in Florida had been dated to >5000 calendar years B.P. (Middle Archaic), but the data were not conclusive and the antiquity of the sites remained in doubt (*4, 5*).

In the 1990s, four additional mound sites in Louisiana (*6–8*) and two in Florida (*8*) have been identified as Middle Archaic in age. Collectively, the Middle Archaic mound sites provide 56 radiometric dates that establish the antiquity of earthen mounds in the southeast. Of these sites, Watson Brake in northeast Louisiana is the largest, most complex, and most securely dated site. Its 11 mounds and connecting ridges form an oval-shaped earthen enclosure 280 m in diameter (Fig. 1). The largest mound (Gentry Mound) is 7.5 m high; the other mounds measure between 4.5 and 1 m in height, and the connecting ridges average 1 m in height. Here we present evi-

J. W. Saunders, G. L. Stringer, R. Jones, Department of Geosciences, Northeast Louisiana University, Monroe, LA 71209, USA.
R. D. Mandel, Department of Geography, University of Kansas, Lawrence, KS 66045–2121, USA.
R. T. Saucier, 4325 Winchester Road, Vicksburg, MS 39180–8969, USA.
E. T. Allen, Natural Resources Conservation Service, 1605 Arizona Street, Monroe, LA 71202–3697, USA.
C. T. Hallmark, Soil and Crop Sciences Department, Texas A&M University, College Station, TX 77843–2474, USA.
J. K. Johnson, Department of Sociology and Anthropology, University of Mississippi, University, MS 38677, USA.
E. H. Jackson, Department of Sociology and Anthropology, University of Southern Mississippi, Box 5074, Hattiesburg, MS, 39406–5074, USA.
C. M. Allen, Department of Biology, Northeast Louisiana University, Monroe, LA 71209, USA.
D. S. Frink, Archaeology Consulting Team, Inc., Post Office Box 145, Essex Junction, VT 05453, USA.
J. K. Feathers, TL Dating, DH-05 Anthropology, University of Washington, Seattle, WA 98195, USA.
S. Williams, Post Office Box 22354, Santa Fe, NM 87502–2354, USA.
K. J. Gremillion, Department of Anthropology, Ohio State University, 244 Lord Hall, 214 West 17 Avenue, Columbus, OH 43210–1364, USA.
M. F. Vidrine, Division of Sciences, Louisiana State University at Eunice, Post Office Box 1129, Eunice, LA 70535, USA.
*To whom correspondence should be addressed.

Solvophobically Driven Folding of Nonbiological Oligomers

James C. Nelson, Jeffery G. Saven, Jeffrey S. Moore and Peter G. Wolynes

Science **277** (5333), 1793-1796.
DOI: 10.1126/science.277.5333.1793